Temperature change in subtropical southeastern Africa during the past 790,000 yr

Manuel Chevalier, Brian M. Chase, Lynne J Quick, Lydie Dupont, Thomas Johnson

Temperature change in subtropical southeastern Africa during the past 790,000 yr

Manuel Chevalier[1], Brian M. Chase[2,3], Lynne J. Quick[4], Lydie M. Dupont[5] and Thomas C. Johnson[6]

[1]Institute of Earth Surface Dynamics, University of Lausanne, Géopolis, 1015 Lausanne, Switzerland
[2]Institut des Sciences de l'Evolution–Montpellier (ISEM), Université de Montpellier, Centre National de la Recherche Scientifique (CNRS), EPHE, IRD, 34095 Montpellier, France
[3]Department of Environmental and Geographical Science, University of Cape Town, South Lane, Upper Campus, 7701 Rondebosch, South Africa
[4]African Centre for Coastal Palaeoscience, Nelson Mandela University, 6031 Port Elizabeth, South Africa
[5]MARUM–Center for Marine Environmental Sciences, University of Bremen, Bremen 28359, Germany
[6]Department of Geosciences, University of Massachusetts–Amherst, Amherst, Massachusetts 01003, USA

ABSTRACT

Across the glacial-interglacial cycles of the late Pleistocene (~700 k.y.), temperature variability at low latitudes is often considered to have been negligible compared to changes in precipitation. However, a paucity of quantified temperature records makes this difficult to reliably assess. In this study, we used the Bayesian method CREST (Climate REconstruction SofTware) to produce a 790,000 yr quantified temperature reconstruction from a marine pollen record from southeast Africa. The results reveal a strong similarity between temperature variability in subtropical Africa and global ice volume and CO_2 concentrations, indicating that temperature in the region was not controlled by local insolation, but followed global trends at these time scales, with an amplitude of ~4 °C between glacial minima and interglacial maxima. The data also enabled us to make an assessment of the impact of temperature change on pollen diversity, with results showing there is no link between glacial-age temperatures/ CO_2 and a loss of diversity in this record.

INTRODUCTION

Hydrological conditions have been shown to be highly variable during the late Pleistocene in tropical and subtropical southeastern Africa (e.g., Schefuß et al., 2011; Johnson et al., 2016; Caley et al., 2018). In contrast, relatively little is known about past temperature variability. While some studies have shown that regional temperatures at the end of the last glacial period were 3.5–5.2 °C colder than present day (Kulongoski and Hilton, 2004; Chevalier and Chase, 2015; Johnson et al., 2016), the drivers of temperature changes over time remain unknown. Yet, accounting for temperature is crucial to interpret paleohydrological proxy records in terms of rainfall changes and climate dynamics, as temperature can modulate the net effect of precipitation through evapotranspiration (Chevalier and Chase, 2016; Scheff et al., 2017). Because many proxies used to infer past hydrological change (e.g., lake levels or $\delta^{13}C$ from leaf-wax *n*-alkanes in plants) principally reflect environmental water availability and not rainfall amount per se, the absence of long and detailed temperature records restricts our ability to fully characterize past precipitation amount as a distinct variable.

Unfortunately, few proxies have the capacity to record temperature variability directly (Nicholson et al., 2013), and the trends, amplitude, and drivers of past temperature changes in southern Africa remain elusive. While some fossil pollen taxa are temperature-sensitive, methodological constraints generally limit interpretations to qualitative assessments (e.g., Dupont et al., 2011; Valsecchi et al., 2013). The development of the Bayesian climate reconstruction method CREST (Climate REconstruction SofTware) has enabled the reconstruction of quantified records of past climate change from fossil pollen data (Chevalier et al., 2014), with recent results highlighting a strong connection between terrestrial temperatures and sea-surface temperatures (SSTs) from the Mozambique Channel (Truc et al., 2013; Chevalier and Chase, 2015). However, these reconstructions are too short (20 k.y. and 45 k.y., respectively) to determine responses to a more complete suite of Pleistocene conditions, particularly periods of high eccentricity, when variations in direct insolation were substantially greater than during the last 50 k.y. (Laskar et al., 2004).

Here, we used a pollen record from marine core MD96–2048 (south of the mouth of the Limpopo River; Dupont et al., 2019) as the basis for a quantified reconstruction of temperature variability for the Limpopo River catchment during the last 790 k.y. Pollen data show a strong response of vegetation to glacial-interglacial cycles, with glacial landscapes being dominated by Ericaceae and other montane shrubs, and interglacials dominated by increased forest development (Dupont et al., 2019). These large changes allowed us to determine temperature variability at what is today the southeastern edge of the African monsoon domain (Wang and Ding, 2008) and investigate the relationship with the patterns of climate change that have characterized the late Pleistocene.

MATERIALS AND METHODS
CREST Method

The CREST method is a Bayesian approach that combines presence-only plant occurrence data with modern climatological data to estimate the conditional responses of pollen taxa to specific climate variables, such as mean annual temperature (MAT) (Chevalier et al., 2014; Chevalier, 2019). Defined as probability density functions (PDFs), the taxon-climate response curves are fitted in two steps to incorporate the taxonomic resolution of pollen taxa (most commonly identified at the genus or family level; Fig. 1). First, Gaussian PDFs are fitted for all
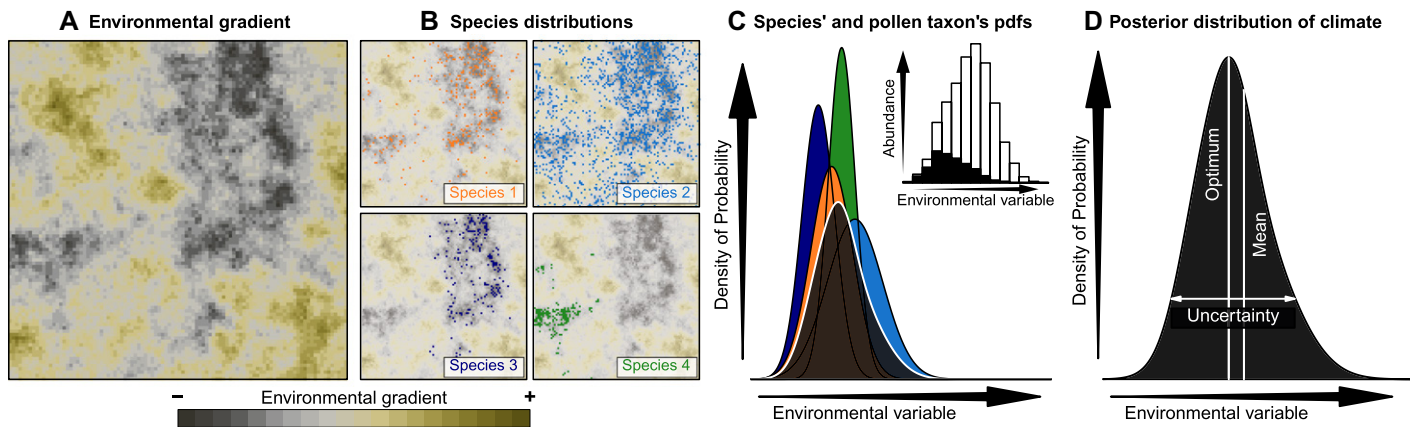
Figure 1. Conceptual representation of the fitting of probability density functions (PDFs) using randomly generated data. (A) Modern distribution of the environmental variable of interest. (B) Modern distribution of four species producing undifferentiated pollen grains in the environment. (C) Four colored curves represent four species PDFs as represented in B, and black PDF represents response of pollen type as a whole. Inset histogram represents distribution of modern environment (white) that is occupied by at least one of the four species of interest (black), highlighting the preference for lower values. (D) Representation of statistics (optimum, mean, and width/uncertainty) that can be measured from each PDF to derive climate estimate.
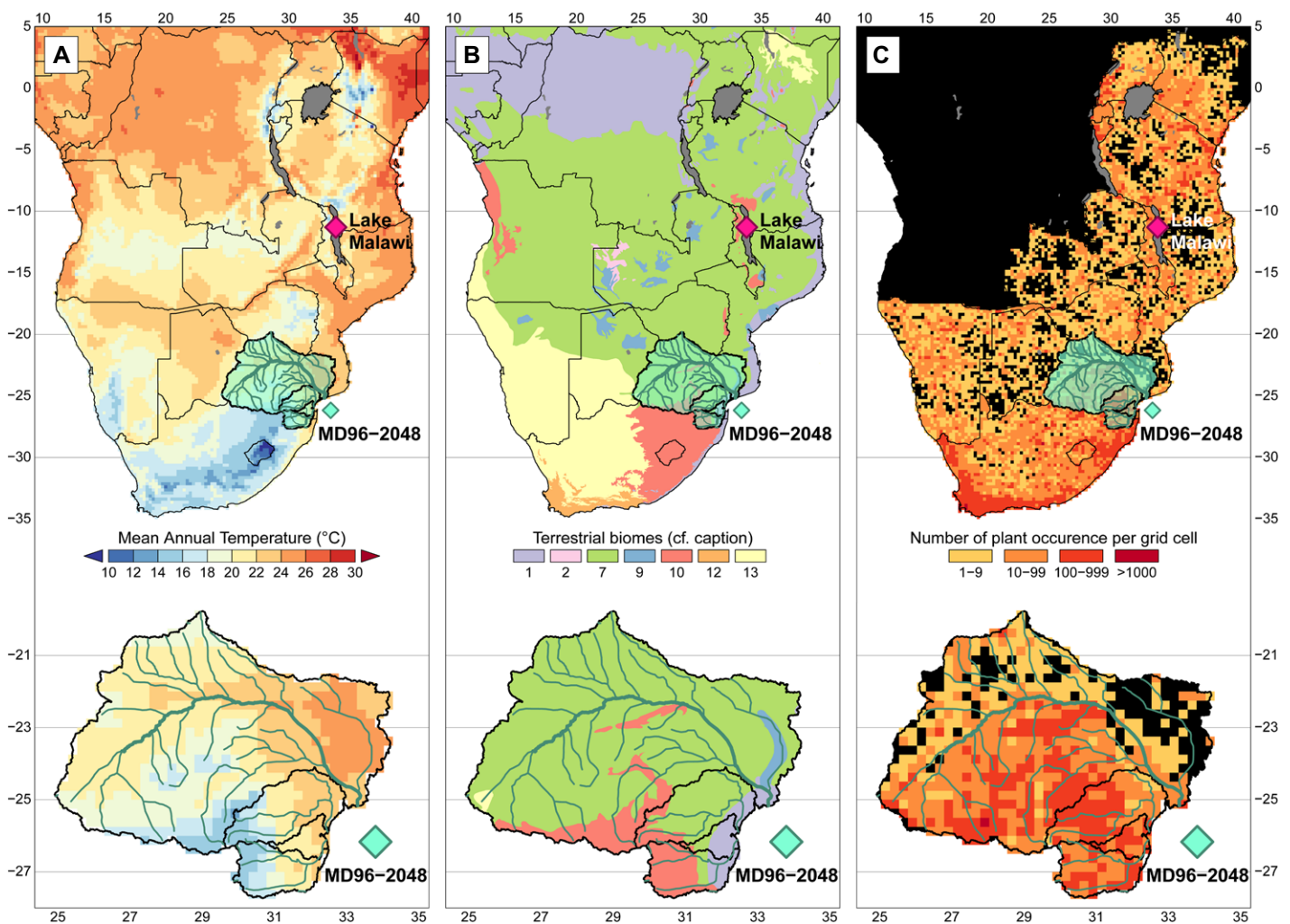

Figure 2. Regional settings. Marine core MD96−2048 (26.1667°S, 34.0167°E) is represented by green diamond. Its catchment is represented in same color. (A) Distribution of mean annual temperature (MAT) across study area (Fick and Hijmans, 2017). (B) Distribution of major terrestrial biomes across same region. 1—Tropical and subtropical moist broadleaf forests; 2—(sub)tropical dry broadleaf forests; 7—(sub)tropical grasslands, savannas, and shrublands, 9—flooded grasslands and savannas, 10—montane grasslands and shrublands, 12—Mediterranean forests, woodlands, and scrub or sclerophyll forests, and 13—deserts and xeric shrublands (Olson et al., 2001). (C) Subset of GBIF (Global Biodiversity Information Facility, https://www.gbif.org/) calibration data set used in this study to fit probability density functions (PDFs; v5; 0.25° grid cell resolution, 324,270 distinct plant occurrences; Chevalier, 2018).

the species that produce the same type of pollen grains from all the climate values corresponding to the presence records (Figs. 1A and 1B). The influence of the heterogeneously distributed modern climate space is removed by weighting each climate value by the inverse of its abundance in the study area (Bray et al., 2006). Species PDFs are then combined to create a higher-order PDF that represents the climate response of the pollen type as a unit (Fig. 1C).

Past MAT values are estimated from the weighted multiplication of the pollen PDFs. Here, the raw percentages of each individual taxon were normalized by the average of the percentages observed in the fossil pollen sequence when the taxon was present to account for taphonomic processes and different pollen production rates. A value higher (lower) than one suggests that the climate at the time of deposition was more (less) favorable than the average climate in which the taxon has been observed during the studied period (Chevalier et al., 2014). The multiplication of the PDFs results in a posterior distribution of probabilities, from which climate estimates and uncertainties are derived (Fig. 1D).

Pollen Record for Marine Core MD96–2048

Located south of the mouth of the Limpopo River (34.0167°E, 26.1667°S, 660 m water depth), marine core MD96–2048 consists of sediments from the catchments of the Limpopo,

Maputo, and Incomati Rivers (>460,000 km²; Fig. 2; Dupont et al., 2011, 2019). The record spans the past 790 k.y., recording over eight complete glacial-interglacial cycles since marine isotope stage (MIS) 20. The resolution of the record varies with a mean resolution of ~3.0 k.y. over the past 342 k.y., and ~6.7 k.y. for the older section. As such, this record is unlikely to have recorded cyclicities with a period shorter than at least 15–20 k.y. Today, the MAT values encompassed by the catchments are fairly homogeneous (mean modern temperature ~20.9 °C, σ = 2.5 °C; Fig. 2A). The large elevational range across the catchment (up to 2000 m in the Drakensberg region in the south, 500–1000 m on the African plateau to the west, and 0–200 m in the east) fosters a range vegetation types (four distinct biomes; Fig. 2B). We refer the reader to Dupont et al. (2011) for a more detailed description of the catchment.

To enable the reconstruction of potentially large vegetation and climatic changes, the calibration data set was designed to include a much broader area than the current catchment size (Fig. 2C), covering a temperature gradient of more than 24 °C and encompassing seven different biomes. Central Africa was not included because the distributions of plant presence records are too fragmentary in the area to estimate reliable PDFs (Chevalier, 2019). Of the 231 terrestrial and aquatic pollen taxa that have been observed, we used the climate response

of 166 terrestrial taxa to reconstruct MAT (see Appendix S1 in the Supplemental Material[1]).

RESULTS AND DISCUSSION
Representativity of the Reconstruction

Reconstructing climate from marine pollen records can be problematic, because marine sediments can integrate large source areas and may be subject to a range of transport vectors that can vary through time. In the case of MD96–2048, the region is dominated by easterly onshore winds year-round (Tyson and Preston-White, 2000), which is not favorable for eolian pollen transport to the coring location, and studies indicate that most of the terrestrial sediment flux is fluvial in origin (Dupont et al., 2011; Castañeda et al., 2016). The MAT value reconstructed for the most recent pollen

---

[1]Supplemental Material. Appendix S1 (pollen taxa used for the reconstruction), Appendices S2 and S3 (comparison of MAT and pollen diversity with independent regional and global temperature records), and Data Set S1 (MAT reconstructions from marine core MD96-2048). Please visit https://doi.org/10.1130/GEOL.S.12837788 to access the supplemental material, and contact editing@geosociety.org with any questions. The CREST software is accessible from https://chevaliermanuel.wixsite.com/webpage/crest/. The mean annual temperature reconstructions are available at https://doi.pangaea.de/10.1594/PANGAEA.915923. The R scripts used to analyze the data and create the figures are available from https://github.com/mchevalier2/Papers/tree/master/Chevalier_etal_MD962048.
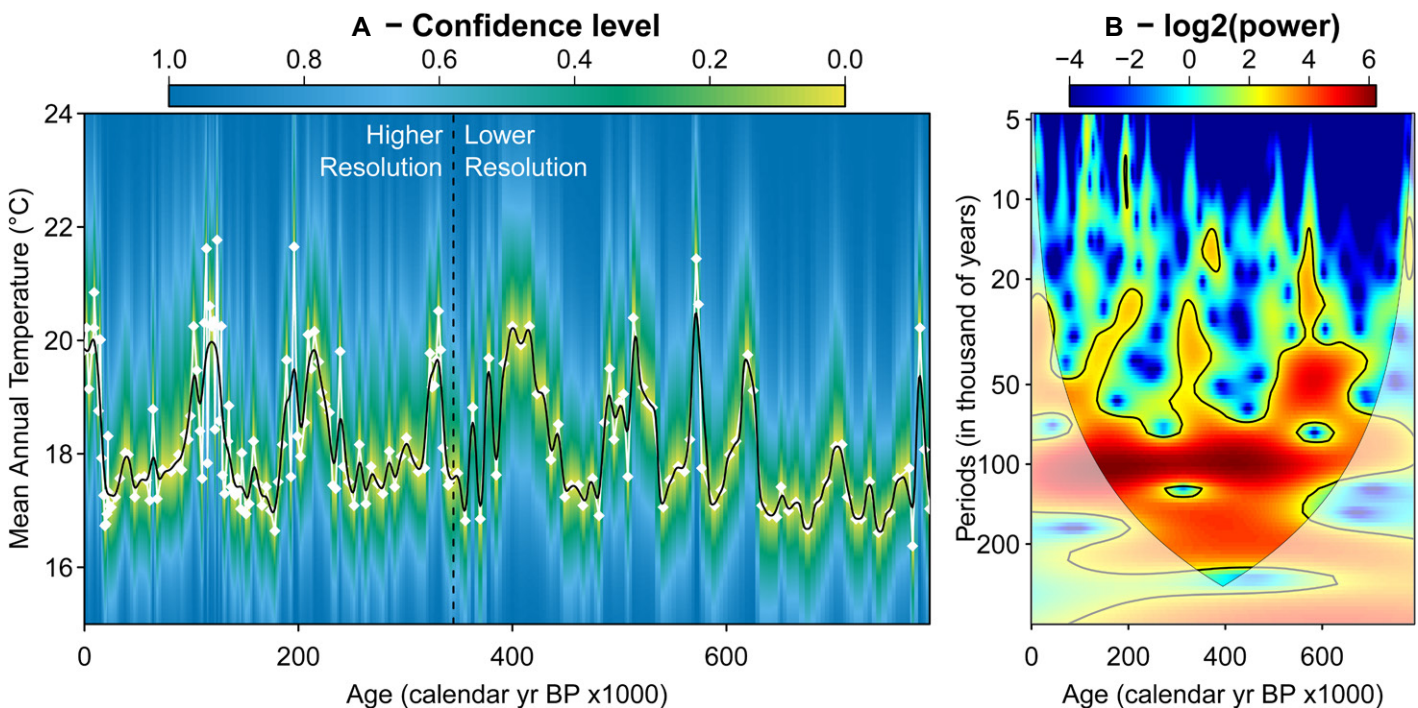

Figure 3. (A) Mean annual temperature (MAT) reconstruction from marine core MD96–2048 (south of the mouth of the Limpopo River, 26.1667°S, 34.0167°E, 660 m water depth). White diamonds represent reconstructed values and have been interpolated using the Gaussian kernel smoothing approach (Rehfeld et al., 2011) as black curve (see details in Appendix S2 [see footnote 1]). Yellow to blue background color gradient represents uncertainties, here expressed as confidence intervals. (B) Continuous Morlet wavelet transform of reconstructions. Panel shows local wavelet power spectrum of record, with black lines indicating cone of influence to show where boundary effects are present and regions of greater than 99% confidence using white-noise model.

sample (19.8 °C, σ = 2.3 °C; Fig. 3) is within the modern value calculated for the catchment as a whole (20.9 °C, σ = 2.5 °C), highlighting the fact that the pollen and associated MAT reconstructions reflect the catchment's average temperature.

Temperature Reconstructions and Global Temperature Forcing

The MD96–2048 MAT reconstruction is strikingly similar to glacial-interglacial signatures of global temperature (Pearson's correlation index ρ = 0.76 [last 342 k.y.]/0.72 [entire record]; Jouzel et al., 2007), atmospheric CO_2 concentration (ρ = 0.77/0.74; Lüthi et al., 2008; Bereiter et al., 2015), and ice volume (ρ = –0.79/–0.66; Lisiecki and Raymo, 2005) throughout the past 790 k.y. (Fig. 4; Appendix S2). These high correlations suggest that temperature variability in southeast Africa is more tightly linked to global temperature changes via glacial and CO_2 feedbacks than to local summer insolation (cf. Herbert et al., 2010).

Maximum interglacial temperatures averaged 21.0 ± 0.7 °C in the last 342 k.y. (20.6 ± 1.1 °C for the entire record), while minimum glacial temperatures averaged 17.0 ± 0.3 °C (16.9 ± 0.2 °C for the entire record). While the temporal resolution of the record masks part of the effective climate variability, an amplitude of change of ~4 °C between full glacials and interglacials in the southeast African lowlands is consistent with reconstructions from the nearby Mozambique Channel (3–4 °C; Sonzogni et al., 1998; Caley et al., 2011) and South Africa (3.5 °C; Chevalier and Chase, 2015), and it has been shown to be strong enough to counterbalance a deficit of ~120 mm of rain and maintain similar humidity levels (Chevalier and Chase, 2016).

Previous regional temperature reconstructions from the region also indicated a strong glacial-interglacial link between continental temperature variability and Indian Ocean SST variability (Chevalier and Chase, 2015; Castañeda et al., 2016). Our findings confirm this coeval variability, as highlighted by a correlation with a SST record from the same marine core (ρ = 0.71 [last 342 k.y.]/0.72 [entire record]; Fig. 4; Caley et al., 2018). The two records differ principally by the decline in glacial SSTs around 350 k.y. ago that is not evident in the pollen-based reconstruction. This shift in the glacial temperatures is also absent from a temperature-index record (ratio of leaf wax long-chain n-alkanes, $C_{31}/[C_{29} + C_{31}]$) derived from the same core by Castañeda et al. (2016) (ρ = 0.67/0.71, after detrending for a long-term aridification trend). This SST shift is only observed in records derived from foraminifera, while other SST proxies do not record a similar trend (Caley et al., 2011). This difference may reflect different taphonomy or,

more likely, different sensitivities (e.g., seasonal vs. annual signals) of the marine and terrestrial microfossils and proxies obtained from the sediment core.

The only other long quantified African terrestrial temperature record spanning several glacial-interglacial cycles comes from Lake Malawi (Fig. 2; Johnson et al., 2016). While the Malawi temperature record (partially tuned to the global benthic δ18O stack; Lisiecki and Raymo, 2005) exhibits clear glacial-interglacial signals, correlation with our reconstruction (ρ = 0.51/0.30) and other temperature records is generally more modest (Appendix S2), possibly highlighting the fact that different drivers govern temperature in these two regions of Africa (mainly tropical influences at Lake Malawi vs. subtropical and extratropical influences across our study area). It is also possible that Lake Malawi temperature estimates are partially influenced by the extreme lake-level variations that have been reconstructed over the past 800 k.y. (>10 lake-level reductions of 500 m or more; Lyons et al., 2015). These were corrected for, but this variability may have also influenced the archaea producing the tetra-ether index of lipids with 86 carbons (TEX_{86}) data used to derive temperature estimates, thus changing the representativity of the record over time (Johnson et al., 2016).

Pollen Diversity Across Glacial-Interglacial Cycles

The MD96–2048 MAT reconstruction enabled us to analyze the ways in which pollen diversity varied under different temperature conditions and associated atmospheric CO_2 levels across glacial-interglacial cycles. Comparing measured pollen diversity (e.g., number of taxa and Margalef's index [species diversity index; Margalef, 1957] in Figure 4) with temperature, we could not isolate systematic links (Appendix S3). While acknowledging that differences exist between pollen diversity and plant species diversity, especially when the record encompasses several biomes (Goring et al., 2013), this absence of correlation suggests that at the spatiotemporal resolution of this study, glacial and interglacial periods supported equally diverse floras. We did observe a significant pattern coherent with the ~400 k.y. cycle of orbital eccentricity, with the low pollen diversity corresponding with high eccentricity (Appendix S3). A negative correlation between pollen diversity and the ~100 k.y. eccentricity cycle also appears possible, particularly during high phases of the 400 k.y. cycle. While a better-resolved record is required before any clear conclusion can be drawn, we infer that the high-amplitude (low-amplitude) variability in seasonal insolation forcing under higher (lower) eccentricity may result in greater (lesser) levels of ecosystem disruption and displacement, and perhaps the
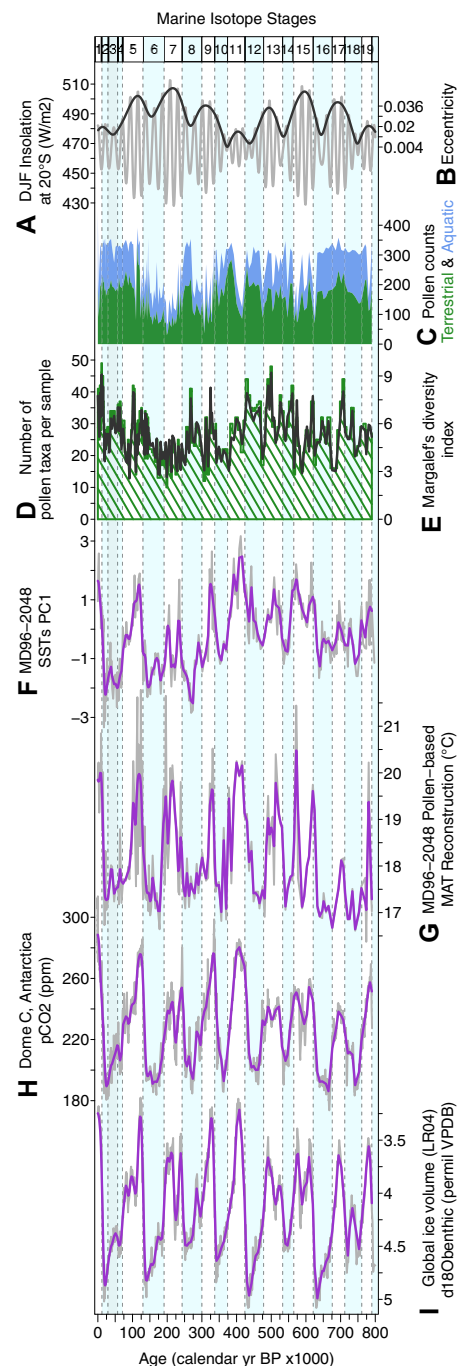

Figure 4. Comparison of our mean annual temperature (MAT) reconstruction (G) with regional and global records: (A) December-January-February (DJF) insolation at 20°S, (B) eccentricity (Laskar et al., 2004), (C) number of pollen grains of terrestrial (green) and aquatic (blue) taxa (Dupont et al., 2019), (D) number of terrestrial pollen taxa per sample (green), (E) Margalef's diversity index (Margalef, 1957), (F) sea-surface temperature (SST) reconstruction derived from the same core (Caley et al., 2018), (H) global atmospheric CO_2 concentration (Bereiter et al., 2015), and (I) global stack of stable oxygen isotopes of benthic foraminifers, LR04 (Lisiecki and Raymo, 2005). VPDB—Vienna Peedee belemnite. Records in gray have been interpolated (purple lines) using Gaussian kernel smoothing approach.

establishment of more diverse vegetations under more stable climatic conditions.

CONCLUSION

Our reconstruction of MAT from fossil pollen data demonstrated the potential of CREST to reconstruct climate on long time scales and reveal past climate variability from low latitudes. Here, we have shown the existence of a strong link between southeast African and global temperatures that indicates that temperature variability in southeast Africa is primarily paced by glacial-interglacial cycles. Temperature changes of 4 °C between glacial and interglacial periods are likely to have had a significant impact on water availability in the region, and these findings reinforce the need to consider temperature as an important and independent driver of tropical climate while interpreting moisture-related proxy records.

REFERENCES CITED

Bereiter, B., Eggleston, S., Schmitt, J., Nehrbass-Ahles, C., Stocker, T.F., Fischer, H., Kipfstuhl, S., and Chappellaz, J., 2015, Revision of the EPICA Dome C CO_2 record from 800 to 600 kyr before present: Geophysical Research Letters, v. 42, p. 542–549, https://doi.org/10.1002/2014GL061957.

Bray, P.J., Blockley, S.P.E., Coope, G.R., Dadswell, L.F., Elias, S.A., Lowe, J.J., and Pollard, A.M., 2006, Refining mutual climatic range (MCR) quantitative estimates of palaeotemperature using ubiquity analysis: Quaternary Science Reviews, v. 25, p. 1865–1876, https://doi.org/10.1016/j.quascirev.2006.01.023.

Caley, T., et al., 2011, High-latitude obliquity as a dominant forcing in the Agulhas current system: Climate of the Past, v. 7, p. 1285–1296, https://doi.org/10.5194/cp-7-1285-2011.

Caley, T., et al., 2018, A two-million-year-long hydroclimatic context for hominin evolution in southeastern Africa: Nature, v. 560, p. 76–79, https://doi.org/10.1038/s41586-018-0309-6.

Castañeda, I.S., Caley, T., Dupont, L.M., Kim, J.-H., Malaizé, B., and Schouten, S., 2016, Middle to late Pleistocene vegetation and climate change in subtropical southern East Africa: Earth and Planetary Science Letters, v. 450, p. 306–316, https://doi.org/10.1016/j.epsl.2016.06.049.

Chevalier, M., 2018, GBIF database for CREST: https://doi.org/10.6084/m9.figshare.6743207 (accessed January 2020).

Chevalier, M., 2019, Enabling possibilities to quantify past climate from fossil assemblages at a global scale: Global and Planetary Change, v. 175, p. 27–35, https://doi.org/10.1016/j.gloplacha.2019.01.016.

Chevalier, M., and Chase, B.M., 2015, Southeast African records reveal a coherent shift from high- to low-latitude forcing mechanisms along the East African margin across last glacial-interglacial transition: Quaternary Science Reviews, v. 125, p. 117–130, https://doi.org/10.1016/j.quascirev.2015.07.009.

Chevalier, M., and Chase, B.M., 2016, Determining the drivers of long-term aridity variability: A southern African case study: Journal of Quaternary Science, v. 31, p. 143–151, https://doi.org/10.1002/jqs.2850.

Chevalier, M., Cheddadi, R., and Chase, B.M., 2014, CREST (Climate REconstruction SofTware): A probability density function (PDF)–based quantitative climate reconstruction method: Climate of the Past, v. 10, p. 2081–2098, https://doi.org/10.5194/cp-10-2081-2014.

Dupont, L.M., Caley, T., Kim, J.-H., Castañeda, I.S., Malaizé, B., and Giraudeau, J., 2011, Glacial-interglacial vegetation dynamics in south eastern Africa coupled to sea surface temperature variations in the western Indian Ocean: Climate of the Past, v. 7, p. 1209–1224, https://doi.org/10.5194/cp-7-1209-2011.

Dupont, L.M., Caley, T., and Castañeda, I.S., 2019, Effects of atmospheric CO_2 variability of the past 800 kyr on the biomes of southeast Africa: Climate of the Past, v. 15, p. 1083–1097, https://doi.org/10.5194/cp-15-1083-2019.

Fick, S.E., and Hijmans, R.J., 2017, WorldClim 2: New 1-km spatial resolution climate surfaces for global land areas: International Journal of Climatology, v. 37, p. 4302–4315, https://doi.org/10.1002/joc.5086.

Goring, S.J., Lacourse, T., Pellatt, M.G., and Mathewes, R.W., 2013, Pollen assemblage richness does not reflect regional plant species richness: A cautionary tale: Journal of Ecology, v. 101, p. 1137–1145, https://doi.org/10.1111/1365-2745.12135.

Herbert, T.D., Peterson, L.C., Lawrence, K.T., and Liu, Z., 2010, Tropical ocean temperatures over the past 3.5 million years: Science, v. 328, p. 1530–1534, https://doi.org/10.1126/science.1185435.

Johnson, T.C., et al., 2016, A progressively wetter climate in southern East Africa over the past 1.3 million years: Nature, v. 537, p. 220–224, https://doi.org/10.1038/nature19065.

Jouzel, J., et al., 2007, Orbital and millennial Antarctic climate variability over the past 800,000 years: Science, v. 317, p. 793–796, https://doi.org/10.1126/science.1141038.

Kulongoski, J.T., and Hilton, D.R., 2004, Climate variability in the Botswana Kalahari from the late Pleistocene to the present day: Geophysical Research Letters, v. 31, L10204, https://doi.org/10.1029/2003GL019238.

Laskar, J., Robutel, P., Joutel, F., Gastineau, M., Correia, A.C.M., and Levrard, B., 2004, A long-term numerical solution for the insolation quantities of the Earth: Astronomy & Astrophysics, v. 428, p. 261–285, https://doi.org/10.1051/0004-6361:20041335.

Lisiecki, L.E., and Raymo, M.E., 2005, A Pliocene–Pleistocene stack of 57 globally distributed benthic $\delta^{18}O$ records: Paleoceanography, v. 20, PA1003, https://doi.org/10.1029/2004PA001071.

Lüthi, D., et al., 2008, High-resolution carbon dioxide concentration record 650,000–800,000 years before present: Nature, v. 453, p. 379–382, https://doi.org/10.1038/nature06949.

Lyons, R.P., et al., 2015, Continuous 1.3-million-year record of East African hydroclimate, and implications for patterns of evolution and biodiversity: Proceedings of the National Academy of Sciences of the United States of America, v. 112, p. 15568–15573, https://doi.org/10.1073/pnas.1512864112.

Margalef, D.R., 1957, Information theory in ecology: Memorias de la Real Academia de Ciencias y Artes de Barcelona, v. 32, p. 374–559, https://ci.nii.ac.jp/naid/10011534559/en/.

Nicholson, S.E., Nash, D.J., Chase, B.M., Grab, S.W., Shanahan, T.M., Verschuren, D., Asrat, A., Lézine, A.-M., and Umer, M., 2013, Temperature variability over Africa during the last 2000 years: The Holocene, v. 23, p. 1085–1094, https://doi.org/10.1177/0959683613483618.

Olson, D.M., et al., 2001, Terrestrial ecoregions of the world: A new map of life on Earth: A new global map of terrestrial ecoregions provides an innovative tool for conserving biodiversity: Bioscience, v. 51, p. 933, https://doi.org/10.1641/0006-3568(2001)051[0933:TEOTWA]2.0.CO;2.

Rehfeld, K., Marwan, N., Heitzig, J., and Kurths, J., 2011, Comparison of correlation analysis techniques for irregularly sampled time series: Nonlinear Processes in Geophysics, v. 18, p. 389–404, https://doi.org/10.5194/npg-18-389-2011.

Scheff, J., Seager, R., Liu, H., and Coats, S., 2017, Are glacials dry? Consequences for paleoclimatology and for greenhouse warming: Journal of Climate, v. 30, p. 6593–6609, https://doi.org/10.1175/JCLI-D-16-0854.1.

Schefuß, E., Kuhlmann, H., Mollenhauer, G., Prange, M., and Pätzold, J., 2011, Forcing of wet phases in southeast Africa over the past 17,000 years: Nature, v. 480, p. 509–512, https://doi.org/10.1038/nature10685.

Sonzogni, C., Bard, E., and Rostek, F., 1998, Tropical sea-surface temperatures during the last glacial period: A view based on alkenones in Indian Ocean sediments: Quaternary Science Reviews, v. 17, p. 1185–1201, https://doi.org/10.1016/S0277-3791(97)00099-1.

Truc, L., Chevalier, M., Favier, C., Cheddadi, R., Meadows, M.E., Scott, L., Carr, A.S., Smith, G.F., and Chase, B.M., 2013, Quantification of climate change for the last 20,000 years from Wonderkrater, South Africa: Implications for the long-term dynamics of the Intertropical Convergence Zone: Palaeogeography, Palaeoclimatology, Palaeoecology, v. 386, p. 575–587, https://doi.org/10.1016/j.palaeo.2013.06.024.

Tyson, P.D., and Preston-White, R.A., 2000, The Weather and Climate of Southern Africa (A. Attwell, ed.): Cape Town, South Africa, Oxford University Press–Southern Africa, 408 p.

Valsecchi, V., Chase, B.M., Slingsby, J.A., Carr, A.S., Quick, L.J., Meadows, M.E., Cheddadi, R., and Reimer, P.J., 2013, A high resolution 15,600-year pollen and microcharcoal record from the Cederberg Mountains, South Africa: Palaeogeography, Palaeoclimatology, Palaeoecology, v. 387, p. 6–16, https://doi.org/10.1016/j.palaeo.2013.07.009.

Wang, B., and Ding, Q., 2008, Global monsoon: Dominant mode of annual variation in the tropics: Dynamics of Atmospheres and Oceans, v. 44, p. 165–183, https://doi.org/10.1016/j.dynatmoce.2007.05.002.

Printed in USA